European Radiology (2019) 29:1855–1862
https://doi.org/10.1007/s00330-018-5769-4

MUSCULOSKELETAL

Evaluation of osseous cervical foraminal stenosis in spinal radiculopathy using susceptibility-weighted magnetic resonance imaging

Guenther Engel[1] · Yvonne Y. Bender[1] · Lisa C. Adams[1] · Sarah M. Boker[1] · Ute L. Fahlenkamp[1] · Moritz Wagner[1] · Gerd Diederichs[1] · Bernd Hamm[1] · Marcus R. Makowski[1]

Received: 3 June 2018 / Revised: 23 August 2018 / Accepted: 14 September 2018 / Published online: 15 October 2018
© European Society of Radiology 2018

Abstract

Objective The aim of this study was to evaluate the diagnostic performance of susceptibility-weighted magnetic resonance imaging (SW-MRI) for the evaluation of osseous foraminal stenosis (FS) of the cervical spine compared to conventional MRI-sequences, using computed tomography (CT) as a reference standard.

Materials and methods Twenty-one patients with suspected radiculopathy of the cervical spine were prospectively included. CT and MRI data sets were available for all patients. As standard of reference, 280 neuroforamina of the cervical spine, including 58 foraminal stenosis, were identified on sagittal CT images. T1-, T2-, and SW-MRI of the cervical spine were performed. The presence of foraminal stenosis was assessed on sagittal views in all sequences. Sensitivity and specificity were calculated and differences in detection rate and severity scoring of foraminal stenosis between the different sequences were tested. CT was used as reference standard for all analysis.

Results Fifty-six of 58 osseous foraminal stenosis could be correctly identified on SW-MR magnitude images. SW-MRI achieved a sensitivity of 96.6% and specificity of 99.5% for the identification of foraminal stenosis. In comparison, conventional T1-weighted MRI sequences achieved a sensitivity and specificity of 43.1% and 100% respectively. T2-weighted MRI sequences achieved a sensitivity and specificity of 65.5% and 99.1%, respectively. The overall detection rate was significantly ($p < 0.05$) higher on SW-MRI and there was no significant difference ($p > 0.05$) in severity scoring compared to CT. T1- and T2-weighted MRI underestimated the degree of foraminal stenosis. Intermodality and interobserver agreements were highest for SW-MRI.

Conclusions SW-MRI enables the reliable detection of osseous foraminal stenosis of the cervical spine in patients with spinal radiculopathy with a higher sensitivity compared to conventional T1- and T2-MRI sequences, with CT as a reference standard.

Key Points

- *Susceptibility-weighted magnetic resonance imaging enables the reliable detection of osseous foraminal stenosis of the cervical spine with CT as a reference standard.*
- *This could be relevant for younger patients in order to prevent unnecessary radiation exposure.*
- *This may also facilitate a one-stop-shop approach and speed up diagnostic work-up.*

Keywords Magnetic resonance imaging · Diagnostic imaging · Spine · Radiculopathy

Abbreviations

CT	Computed tomography
FOV	Field of view
GRE	Gradient echo
MEDIC	Multi echo data image combination
MR	Magnetic resonance
MRI	Magnetic resonance imaging
MSK	Musculoskeletal
SD	Standard deviation
STIR	Short tau inversion recovery
SW-MRI	Susceptibility-weighted magnetic resonance imaging
TE	Echo time
TR	Repetition time
TSE	Turbo spin echo

Guenther Engel and Yvonne Y. Bender contributed equally to this work.

✉ Guenther Engel
guenther.engel@charite.de

[1] Department of Radiology, Charité – University Medicine Berlin, Charitéplatz 1, 10117 Berlin, Germany

Introduction

Cervical radiculopathy is one of the most common symptoms of degenerative changes of the cervical spine and ordinarily caused by cervical spondylosis and posterolateral intervertebral disc herniation [20]. Conservative management of cervical radiculopathy improves symptoms in most patients and is usually attempted. Nonetheless, surgery can be required when conservative management fails and symptoms such as pain, paresthesia, sensory loss, or progressive weakness with motor dysfunction occur [8]. However, there is no generally accepted consensus regarding the indications for surgery in patients with cervical radiculopathy [2, 4, 18]. The overlap of symptoms with adjacent dermatomes makes imaging, in addition to clinical examinations, frequently necessary to identify the cause of cervical radiculopathy. Subsequently, surgical planning is based on the identified cause of cervical radiculopathy.

Radiographs in anterior-posterior and lateral views of the cervical spine are typically acquired. The evaluation of the foramina is usually performed by using oblique radiographs. To evaluate underlying osseous changes of foraminal stenosis, additional computed tomography (CT) scans are in some cases performed preoperatively. However, CT is associated with a limited sensitivity in identifying non-osseous causes of foraminal stenosis.

With its excellent soft tissue resolution and non-invasiveness, magnetic resonance imaging (MRI) is usually the preferred imaging technique for presurgical evaluation of degenerative changes of the spine as disc hydration, spinal canal stenosis, foraminal stenosis, spondylolisthesis, and spinal cord changes. A major advantage of MRI is the absence of ionizing radiation. However, MRI is associated with certain limitations especially with regard to the differentiation of osteophytes and disc calcifications, sensitivity to patient motion [7, 17, 21]. Axial and sagittal MR images were shown to be associated with a low specificity for foraminal lesions [12, 24].

Susceptibility-weighted MRI (SW-MRI) enables the assessment of magnetic susceptibility of tissues including ferromagnetic, paramagnetic, and diamagnetic substances. This novel sequence therefore allows the MRI-based detection of bone minerals as they are diamagnetic. The potential of SW-MRI has mainly been used for the differentiation of intracranial bleeding from calcifications or to identify intracranial veins [10]. More recently, SW-MR imaging has also been used to evaluate calcifications in other regions of the body as for example the prostate gland [1, 23].

The aim of this study was to test the diagnostic performance of SW-MRI for the evaluation of osseous cervical foraminal stenosis compared with conventional MRI sequences, using CT as a reference standard. The MRI-based detection of osseous changes of the cervical spine causing foraminal stenosis has the potential to limit the use of additional conventional radiography or CT with the associated exposure to ionizing radiation.

Material and methods

Study population

Approval for this study was prospectively given from the local ethics review board. Before undergoing the study protocol, written consent was obtained from all subjects. A clinical MRI scan of the cervical spine was required in all subjects. Overall, 280 neuroforamina of 21 subjects with suspected radiculopathy were available for analysis. In addition to the standard sagittal and axial study protocol, a susceptibility-weighted imaging sequence was performed. On average, CT and MRI scans were performed 2.91 ± 3.99 months apart. Only patients in whom CT scans of the cervical spine, performed within the last 12 month, were available were included. Before the MRI examination, patient history was searched for previous CT examinations within the last 12 months or scheduled CT examinations in the near future. Overall, 26 patients could be included initially of which 4 had to be excluded because they were unable to complete the MRI examination due to various reasons (e.g., pain, claustrophobia) and 1 had to be excluded since the MRI examination was in total non-diagnostic due to severe foreign body artifacts (Fig. 1). The study population included 12 female (57.1%, mean age 51.8 ± 13.1) and nine male (42.9%, mean age 53 ± 14.4) subjects who underwent MRI of the cervical spine in our institution.

Imaging protocol

Magnetic resonance imaging was performed on a Siemens 1.5 T scanner (Avanto; Siemens Healthineers AG) in a standardized supine position with a standard neck coil for the cervical spine. The following spine MRI protocol, which is routinely used in our department for the diagnosis of cervical spine lesions, was applied: sagittal T1 TSE, T2 TSE, and axial T2 MEDIC (T1 TSE: field of view [FOV] 240 mm^2, matrix 448, TR/TE = 803/21 ms, 150° flip angle, and 3-mm slice thickness; T2 TSE: FOV 240 mm^2, matrix 448, TR/TE = 2800/77 ms, 150° flip angle, and 3-mm slice thickness). In 4 of the 21 subjects, a sagittal STIR sequence was acquired instead of the regular sagittal T2 TSE STIR TSE: field of view (FOV) 280 mm^2, matrix 320, TR/TE = 4000/30 ms, 150° flip angle, and 3-mm slice thickness. A 3D fast low-angle gradient-echo sequence (SW-MR) was added to the routine spine protocol. Artifacts were minimized by using a standard ventral saturator. SW-MR is based on magnitude and phase images which are reconstructed from the acquired three-dimensional raw data sets [6, 11, 16]. A velocity-compensated 3D-GRE sequence is part of the SW-MRI and comparable to standard GRE sequences for the detection of T2* time-shortening lesions. Phase information grants the differentiation of calcifications and other lesions such as microbleeds or tissue artifacts [3, 6, 11]. Imaging parameters of the SW-MRI sequence

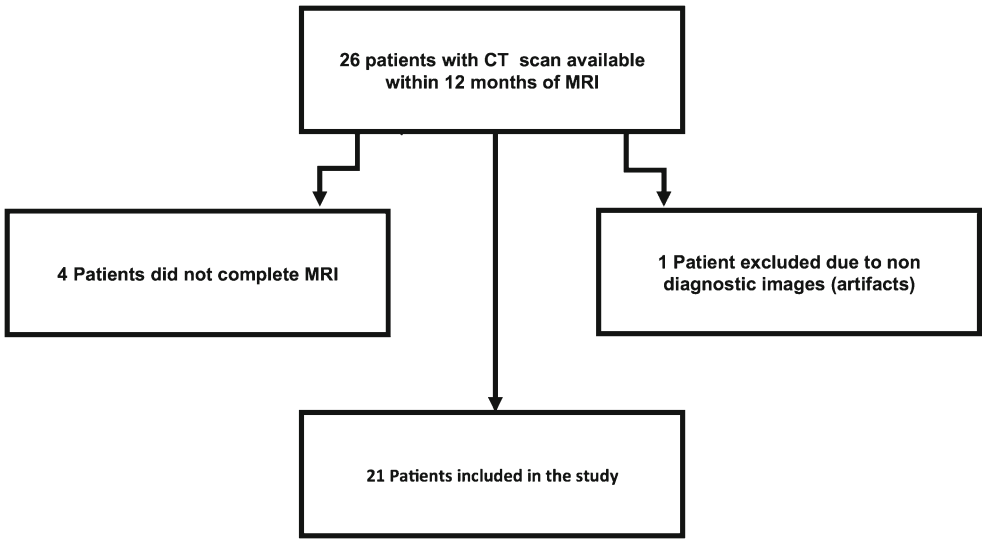

Fig. 1 Flowchart depicting inclusion and exclusion of patients for this study. Initially, 26 patients with suspected spinal radiculopathy that were referred for an MRI of the cervical spine had CT images available. Of these 26, a total of 5 had to be excluded because they either did not complete the MRI examination or the MRI images were non-diagnostic. Overall, 21 patients could be included in this study

were automatically aligned to the sagittal T1/T2-weighted sequences: FOV 240 mm^2, matrix 384, TR/TE 49/14 ms, 15° flip angle, number of phase encoding steps 767, slice thickness 3 mm. Acquisition time for SW-MRI was 5 min and 11 s on average. Clinical standard CT scans of the cervical spine were performed by using a 64- or 128-section Aquilion system (Canon Medical Systems). No changes of protocols were made during this study.

Imaging analysis

SW-MR, MR, and CT images were evaluated using PACS workstations (Centricity Radiology RA1000; GE Healthcare). CT and MR images were interpreted by two observers with experience in MSK radiology: two radiology residents with 5 years and 4 years of diagnostic training respectively, both having 2 years of specific MRI experience. MR images in each sequence as well as CT images were evaluated independently by both reviewers in random order. MR images were read more than 1 week prior to CT images.

A total of 280 foramina in 21 patients were analyzed from C1-2 to C7-T1. Foramina at each level were assessed on both sides. Due to foreign body related magnetic susceptibility artifacts, a total of 14 foramina could not be evaluated and were excluded from the analysis. As a standard of reference, osseous foraminal stenosis of the cervical spine were identified on sagittal CT scans. Window settings were adjusted on sagittal images to identify the nerve root, surrounding perineural fat and osteophytes. Foraminal stenosis were visually detected on sagittal T1- and T2-weighted images based on the shape of the foramen and perineural fat with hyperintense signal in both sequences. A normal foramen was considered to be oval in shape with a harmonious curvature to the bony margins. Osseous changes in degenerative disease of the disc space and the facette joint originated either on the anterior or the posterior margin of the foramen, therefore initially creating a shape similar to the number "8." With progression of the osteophytic changes, it continued to lead towards an occlusion of the foramen. Osteophytes display an isointense signal to the vertebra on conventional T1- and T2-weighted spine MR scans.

On SW-MRI scans, foraminal stenosis were also identified based on the shape of the foramen. Osteophytes were identified based on their cortical and medullary continuity with the vertebral body: hyperintense to the disc and the surrounding adipose tissue on inverse SW-MR magnitude images. Phase images were used to confirm that the hyperintense signal on inverse SW-MR magnitude images related to osseous structures (Figs. 2 and 3). In order to facilitate the interpretation of the phase image, which tends to give poor anatomical detail, an image fusion was performed (Fig. 3).

Additionally, foraminal stenosis was graded by percentage of stenosis, perineural fat obliteration, and changes of the nerve root: "normal" representing no perineural fat obliteration; "mild" representing < 50% stenosis, mild perineural fat obliteration, and no morphological change of nerve root; "moderate" representing > 50% stenosis, moderate perineural fat obliteration without collapse of the nerve root; "severe" representing > 50% stenosis and collapse of the nerve root [13]. Additionally, the sagittal diameter of the foramina was measured in all MRI sequences and CT images.

Statistical analysis

Variables are reported as mean ± standard deviation. Sensitivities and specificities of SW-MRI compared with those of T1- and T2-weighted MRI scans and computed tomography images were computed. Additionally, the rate of detection of CT-confirmed foraminal stenosis of SW-MRI was compared to T1- and T2-weighted sequences using a X^2

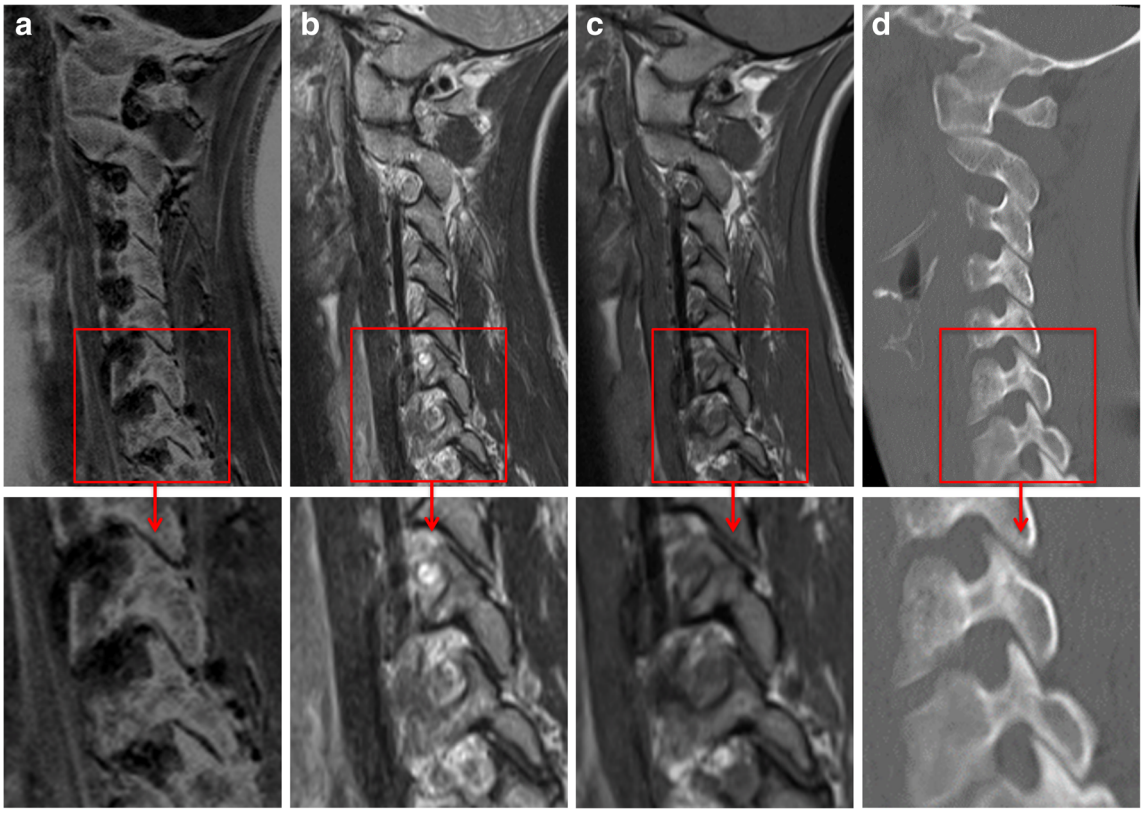

Fig. 2 Example images of a "normal" cervical spine without stenosis of the neuroforamina in sagittal planes. Images show the cervical spine of a 35-year-old woman reporting neck pain. No osseous foraminal stenosis was detected. Facette joint degeneration on the right side was identified as the most likely cause of the clinical symptoms. From left to right: **a** inverted magnitude SW-MR image, **b** T2-weighted MR image, **c** T1-weighted MR image, **d** computed tomography image. Osseous foraminal edges can be clearly delineated on SW-MRI. On T1- and T2-weighted images, the delineation of the neuroforamina was more challenging. Image at the bottom show magnified views of the highlighted segments (red box)

test. The severity score results for computed tomography were compared to those of SW-MRI and T1/T2-weighted MRI scans using Wilcoxon signed rank test. A p value of less than 0.05 was considered statistically significant. Interobserver reliability was tested using Cohen's Kappa and the benchmark scale by Landis and Koch. Intermodality variation for foraminal diameter measurements was assessed using Bland-Altman plots, which were generated to display the spread of data and the limits of agreement. Linear regression was applied to determine the relationship between sagittal diameter measurements on SWI, conventional MRI spine sequences, and CT.

Results

Detection rates for cervical foraminal stenosis

Within the group of 280 cervical neuroforamina, a total of 58 osseous foraminal stenosis detected using computed tomography images of the cervical spine as a reference standard (Figs. 2 and 3). The overall prevalence of osseous foraminal stenosis was 85% in our study population (three subjects showed no detectable stenosis on computed tomography images). On inverted SW-MR magnitude images 57, osseous foraminal stenosis (98.3%) were detected, whereas one stenosis (1.7%) was overdiagnosed and two stenosis were not detected (3.4%).

T1-weighted MRI sequences performed the worst and were only able to detect 25 osseous foraminal stenosis (43.1%), whereas 33 stenosis (56.9%) were not detected. T2-weighted MRI sequences performed better but still not as well as SW-MRI detecting 33 osseous foraminal stenosis (56.9%), while leaving 25 stenosis undetected (43.1%). Overall, the rate of detection for computed tomography confirmed osseous foraminal stenosis was significantly ($p > 0.05$) higher for SW-MRI compared to both T1- and T2-weighted MR sequences (Fig. 4).

Severity scoring of cervical foraminal stenosis

Using the severity score from 0 for no evident stenosis to 3 for more than 50% stenosis with obliteration of perineural fat and collapse of the nerve root, there was a significant difference between the scores attributed on T1- and T2-weighted MR

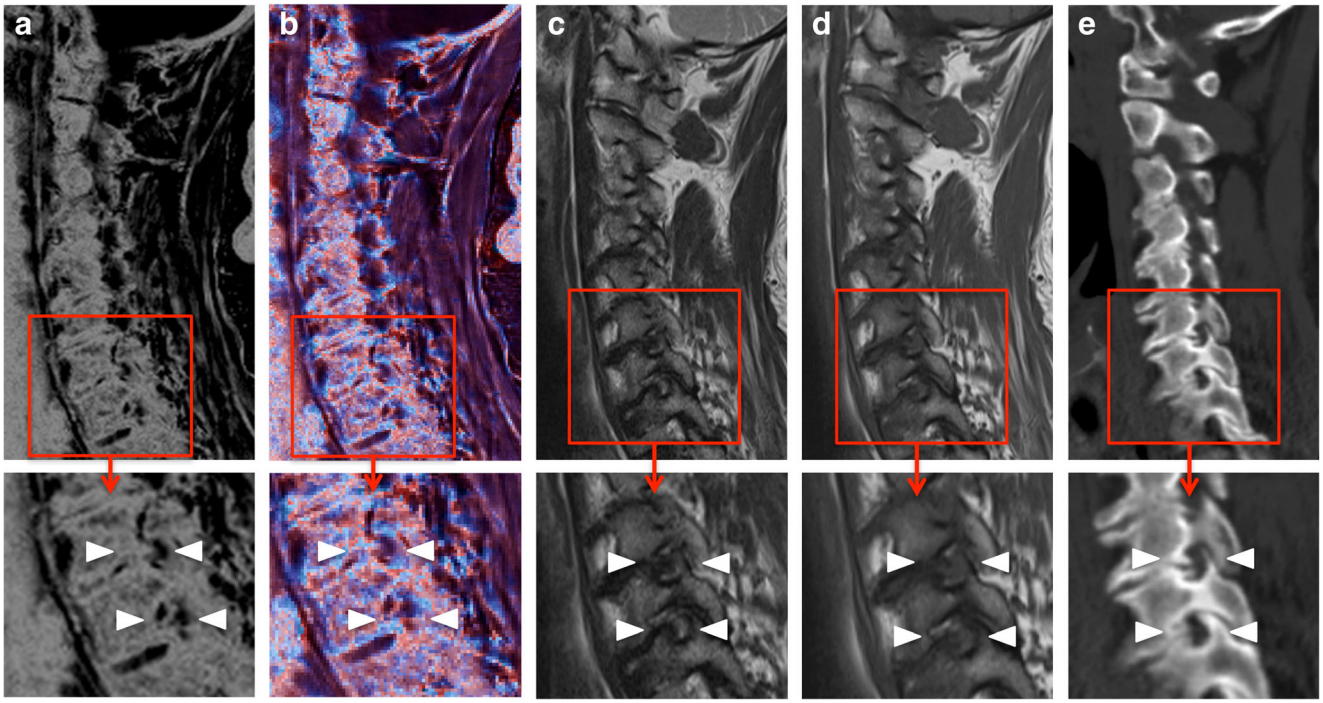

Fig. 3 Example images of neuroforaminal stenosis of the lower cervical spine, sagittal planes. Images show the cervical spine of a 72-year-old man complaining of neck pain, radiating pain, and paresthesia in his right arm. Moderate to severe osseous foraminal stenosis was detected affecting the neuroforamina C6–C8 on the right side, offering a morphological correlate to the clinical symptoms. From left to right: **a** inverted magnitude SW-MR image, **b** fusion image overlaying the phase image onto the inverted magnitude SW-MR image, phase image is color-coded, blue pixels depicting positive phase changes, **c** T2-weighted MR image, **d** T1-weighted MR image, **e** computed tomography image. Red boxes mark segments with neuroforaminal stenosis. Image at the bottom show magnified views of the highlighted segments (red box). White arrowheads point to neuroforaminal stenosis

sequences compared to the computed tomography reference standard (Fig. 5). There was no significant ($p > 0.05$) difference between the attributed scores on SW-MRI compared to computed tomography. The majority of the observed neuroforaminal stenosis were graded as "mild" (grade 1), while a small number were graded as "moderate" or "severe" ($n = 11$). The higher grade stenosis showed a tendency towards an underestimation by T1- and T2-weighted MRI sequences and none of this type of stenosis was detected as being higher grade on T1-weighted MRI sequences and only 3 being accordingly scored on T2-weighted MR sequences. In contrast, SW-MRI correctly identified all of the 11 higher grade foraminal stenosis and overestimated 1 additional "mild" stenosis as "moderate."

Sensitivity and specificity for the detection of cervical foraminal stenosis

The measured sensitivity was significantly ($p \leq 0.05$) higher on SW-MRI compared to conventional T1- and T2-weighted MRI sequences. The measured specificity was comparable and not significantly different ($p > 0.05$) between the three sequence types at close to 100%. SW-MRI achieved a sensitivity of 96.6% and specificity of 99.5% for the detection of osseous foraminal stenosis of the cervical spine with a 95% confidence interval of 0.87–0.99 and 0.97–0.99, respectively. Conventional T1-weighted MRI sequences achieved a sensitivity and specificity of 43.1% and 100%, respectively with 95% confidence intervals of 0.30–0.57 and 0.98–1.00, if computed tomography images were excluded from analysis. Conventional T2-weighted MRI sequences achieved a sensitivity and specificity of 65.5% and 99.1%, with respective 95% confidence intervals ranging from 0.52–0.77 and 0.96–0.99, if blinded to computed tomography images.

Intermodality agreement for diameter measurements of osseous foraminal stenosis

Measurements of the sagittal diameter of foraminal stenosis showed a relatively narrow intermodality variation on SW-MRI compared to the reference standard computed tomography (Fig. 6). Correlation between the two modalities was high with $y = 0.78\times + 0.85$, CI 95% = -0.79–0.93, $R^2 = 0.81$. Meanwhile, the intermodality variation was highest for T1-weighted MRI sequences with $y = 0.41\times + 3.1$, CI 95% = -0.98–2.92, $R^2 = 0.21$. T2-weighted MRI sequences also showed higher variation with $y = 0.62\times + 1.72$, CI 95%= -1.14–1.93, $R^2 = 0.45$.

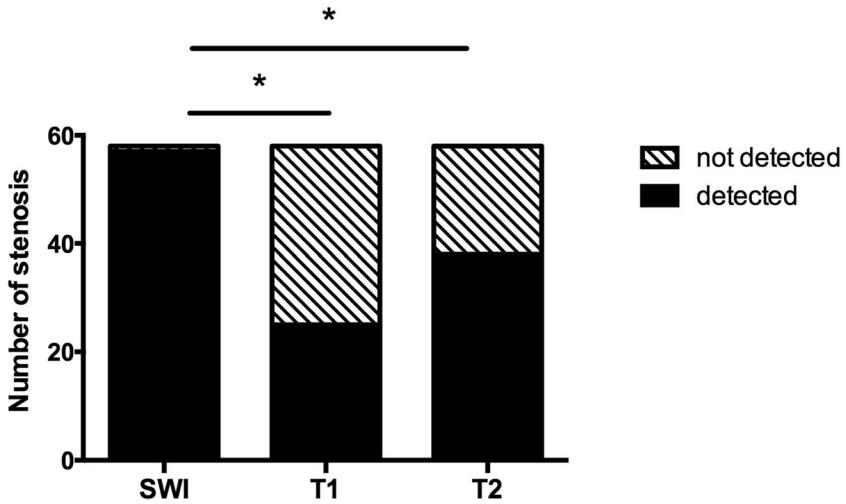

Fig. 4 Detection rate of neuroforaminal stenosis with the different imaging techniques. The represented data demonstrate that SW-MRI enables the detection of significantly ($p < 0.05$) higher number of the neuroforaminal stenosis of the cervical spine, compared to conventional T1- and T2-weighted MRI sequences. All neuroforaminal stenosis were confirmed by the reference standard CT imaging. Detection rate was lowest for T1-weighted MRI sequences. Black bars show number of detected stenosis, shaded parts of bars show number of non-detected stenosis. Stars representing statistically significant difference with $p < 0.05$ based on the X^2 test

Interobserver reliability for detection of osseous foraminal stenosis

The interrater reliability for the reference standard imaging technique computed tomography of the cervical spine was highest according to the benchmark scale by Landis and Koch for the detection of osseous foraminal stenosis with a Kappa value of 0.98. SW-MRI performed comparably with a high agreement and a Kappa value of 0.95. Conventional T1- and T2-weighted MRI sequences still showed a high to immediate agreement and performed significantly ($p \leq 0.05$) worse with a Kappa value of 0.73 for T2-weighted MRI sequences and a Kappa value of 0.66 for T1-weighted MRI sequences.

Discussion

This study demonstrates that SW-MRI enables the reliable detection of osseous foraminal stenosis of the cervical spine in patients with spinal radiculopathy with a higher sensitivity, compared to conventional T1/T2 MR sequences. Specificity values did not differ significantly between the three MR sequence types. Computed tomography (CT) was used as reference standard for all measurements and comparisons. Furthermore, interobserver agreement was higher for SW-MRI compared to T1/T2 MR Sequences. Interobserver agreement for T1/2 MR Sequences in our study was comparable to previous studies on this topic [5, 9]. Intermodality agreement on the diameter of the osseous margins of the foramina and the grading of stenosis between CT and MRI was also highest for SW-MRI.

The current state-of-the-art diagnostic work-up for the detection and treatment-planning for cervical radiculopathy caused by foraminal stenosis typically includes conventional radiography and/or CT imaging to detect and evaluate osseous stenosis and additional MR imaging to detect non-osseous causes for spinal and foraminal stenosis. This usual approach leads to two separate diagnostic appointments and slows down the work-up of the patient. Furthermore, radiation sensitive areas being in close proximity to the area of interest, such as the thyroid gland, can be exposed to ionizing radiation, which is especially relevant in a younger patient collective.

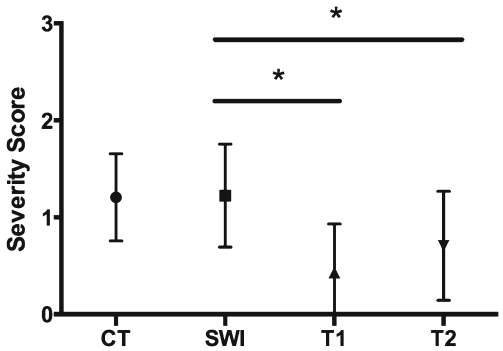

Fig. 5 Severity score of neuroforaminal stenosis with the different imaging techniques. The represented data demonstrate that severity scores attributed on SW-MRI were comparable to the reference standard CT imaging of the cervical spine with no significant difference between the two imaging modalities ($p > 0.05$). In contrast, T1- and T2-weighted MRI sequences showed a significant difference ($p < 0.05$) in scoring and tended to an underestimation of the degree of osseous foraminal stenosis. T1- and T2-weighted sequences show lower severity scores of stenosis compared to computed tomography and SWI. Data shown as mean ± SD. Stars representing statistically significant difference with $p < 0.05$ based on the Wilcoxon signed rank test

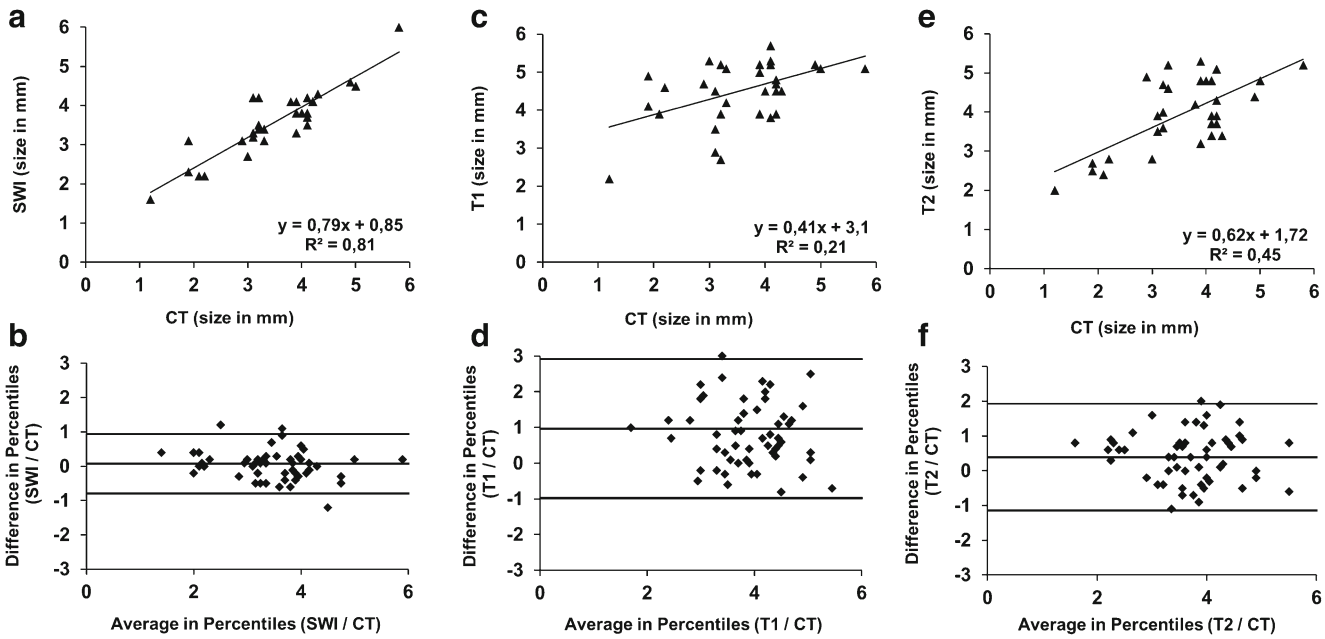

Fig. 6 Intermodality agreement for foraminal stenosis sagittal diameter. Intermodality agreement for foraminal stenosis sagittal diameter between SWI, T1-, and T2-weighted MRI and CT as reference standard. **a**, **b** Diameter measurements showed a strong correlation and agreement for SW-MRI, indicating the good agreement between SWI and CT measurements. **c**, **d** For T1-weighted MRI sequences, the correlation was low and intermodality variation was high, showing a wider confidence interval. **e**, **f** T2-weighted MRI sequences showed a moderate correlation. Bland-Altman plots: centerline, mean absolute difference central line; upper and lower line, limits of agreement (95% confidence intervals)

So far different studies have tested novel approaches to improve the MR-based evaluation of neuroforamina and the associated pathologies [12, 15, 19, 22, 24]. The main limitation of MRI, compared to computed tomography, is however the limited value of MRI for the detection of osteophytic changes as a cause of foraminal stenosis [5, 25]. Standard T1- and T2-weighted MRI sequences do not allow a differentiation of disc herniations, osteophytes, and disc calcifications in standard MRI sequences [7, 17, 21]. In unclear cases, additional CT scans can be required to identify osseous changes and the degree of neuroforaminal stenosis.

Our study demonstrates that osseous foraminal stenosis can be reliably detected on plane sagittal SW-MRI images. Therefore, it can potentially limit the number of required additional CT scans in the future. Especially young patient populations may benefit from potential reduction in ionizing radiation. Furthermore, delays in treatment and costs may be reduced when necessary information regarding osseous and non-osseous causes of foraminal stenosis are obtained with only one imaging modality (one-stop shop). The overall examination time is lengthened by about 5 min, which was well tolerated by all subjects during our study.

Limitations

Limitations of this study include the small sample size. Another limitation of this study is that flexion and extension of the spine influences the shape of the cervical foramen [14], all images have been obtained in a similar supine position. However, positioning was in some cases slightly different during CT imaging. Moreover, some neuroforamina could not be evaluated because of foreign body artifacts due to spinal implants and/or disc replacements or artifacts due to air bubbles in postoperative patients. It has to be noted that SW-MRI is more sensitive towards these types of artifacts than conventional T1/T2 spin echo sequences. Also in four of our patients, the use of STIR images might have an influence on the assessment of the degree of stenosis due to the suppressed fat signal of the perineural fatty tissue. Also, the suppressed fatty tissue results in a lower contrast to the low signal of cortical bone. Furthermore, different interfaces between tissues can cause phase shifts on phase images that can increase the difficulty of image interpretation. Therefore, a certain diagnostic expertise in using this type of sequence needs to be acquired by the image reader.

Conclusion

Susceptibility-weighted magnetic resonance imaging enables the reliable detection of osseous changes causing foraminal stenosis of the cervical spine in patients with spinal radiculopathy with a higher sensitivity compared to conventional T1- and T2-weighted MRI sequences, using CT as a reference standard. Therefore, SW-MRI can be a useful option

to avoid radiation exposure especially in young patients suffering from spinal radiculopathy or in follow-up examinations.

Funding The authors state that this work has not received any funding.

Compliance with ethical standards

Guarantor The scientific guarantor of this publication is Yvonne Y. Bender.

Conflict of interest The authors of this manuscript declare a relationship with Siemens Healthineers AG. Siemens Heathineers AG provided financial and technical support for conducting the study. Siemens Heathineers AG did not have control over the study conduct or data analysis.

Statistics and biometry No complex statistical methods were necessary for this paper.

Informed consent Written informed consent was obtained from all subjects (patients) in this study.

Ethical approval Institutional Review Board approval was obtained.

Methodology
- Prospective
- Diagnostic or prognostic study
- Performed at one institution

References

1. Bai Y, Wang MY, Han YH et al (2013) Susceptibility weighted imaging: a new tool in the diagnosis of prostate cancer and detection of prostatic calcification. PLoS One 8:e53237
2. Caridi JM, Pumberger M, Hughes AP (2011) Cervical radiculopathy: a review. HSS J 7:265–272
3. Cheng AL, Batool S, McCreary CR et al (2013) Susceptibility-weighted imaging is more reliable than T2*-weighted gradient-recalled echo MRI for detecting microbleeds. Stroke 44:2782–2786
4. Eubanks JD (2010) Cervical radiculopathy: nonoperative management of neck pain and radicular symptoms. Am Fam Physician 81:33–40
5. Fu MC, Webb ML, Buerba RA et al (2016) Comparison of agreement of cervical spine degenerative pathology findings in magnetic resonance imaging studies. Spine J 16:42–48
6. Haacke EM, Mittal S, Wu Z, Neelavalli J, Cheng YC (2009) Susceptibility-weighted imaging: technical aspects and clinical applications, part 1. AJNR Am J Neuroradiol 30:19–30
7. Kaiser JA, Holland BA (1998) Imaging of the cervical spine. Spine (Phila Pa 1976) 23:2701–2712
8. Kim KT, Kim YB (2010) Cervical radiculopathy due to cervical degenerative diseases : anatomy, diagnosis and treatment. J Korean Neurosurg Soc 48:473–479
9. Kuijper B, Beelen A, van der Kallen BF et al (2011) Interobserver agreement on MRI evaluation of patients with cervical radiculopathy. Clin Radiol 66:25–29
10. Kurz FT, Freitag M, Schlemmer HP, Bendszus M, Ziener CH (2016) Principles and applications of susceptibility weighted imaging. Radiologe 56:124–136
11. Mittal S, Wu Z, Neelavalli J, Haacke EM (2009) Susceptibility-weighted imaging: technical aspects and clinical applications, part 2. AJNR Am J Neuroradiol 30:232–252
12. Modic MT, Masaryk TJ, Ross JS, Mulopulos GP, Bundschuh CV, Bohlman H (1987) Cervical radiculopathy: value of oblique MR imaging. Radiology 163:227–231
13. Park HJ, Kim SS, Han CH et al (2014) The clinical correlation of a new practical MRI method for grading cervical neural foraminal stenosis based on oblique sagittal images. AJR Am J Roentgenol 203:412–417
14. Park HJ, Kim JH, Lee JW et al (2015) Clinical correlation of a new and practical magnetic resonance grading system for cervical foraminal stenosis assessment. Acta Radiol 1987(56):727–732
15. Park MS, Moon SH, Lee HM et al (2015) Diagnostic value of oblique magnetic resonance images for evaluating cervical foraminal stenosis. Spine J 15:607–611
16. Reichenbach JR, Haacke EM (2001) High-resolution BOLD venographic imaging: a window into brain function. NMR Biomed 14:453–467
17. Reul J, Gievers B, Weis J, Thron A (1995) Assessment of the narrow cervical spinal canal: a prospective comparison of MRI, myelography and CT-myelography. Neuroradiology 37:187–191
18. Rhee JM, Yoon T, Riew KD (2007) Cervical radiculopathy. J Am Acad Orthop Surg 15:486–494
19. Ross JS, Ruggieri PM, Glicklich M et al (1993) 3D MRI of the cervical spine: low flip angle FISP vs. Gd-DTPA TurboFLASH in degenerative disk disease. J Comput Assist Tomogr 17:26–33
20. Ruggieri PM (1995) Cervical radiculopathy. Neuroimaging Clin N Am 5:349–366
21. Shafaie FF, Wippold FJ 2nd, Gado M, Pilgram TK, Riew KD (1999) Comparison of computed tomography myelography and magnetic resonance imaging in the evaluation of cervical spondylotic myelopathy and radiculopathy. Spine 24:1781–1785
22. Simpson AK, Sabino J, Whang P, Emerson JW, Grauer JN (2009) The assessment of cervical foramina with oblique radiographs: the effect of film angle on foraminal area. J Spinal Disord Tech 22:21–25
23. Straub S, Laun FB, Emmerich J et al (2017) Potential of quantitative susceptibility mapping for detection of prostatic calcifications. J Magn Reson Imaging 45:889–898
24. Van de Kelft E, van Vyve M (1994) Diagnostic imaging algorithm for cervical soft disc herniation. J Neurol Neurosurg Psychiatry 57:724–728
25. Yousem DM, Atlas SW, Goldberg HI, Grossman RI (1991) Degenerative narrowing of the cervical spine neural foramina: evaluation with high-resolution 3DFT gradient-echo MR imaging. AJNR Am J Neuroradiol 12:229–236